Removal of Cd (II) and Zn (II) ions from Aqueous Solutions using Carbonized and Functionalized *Persea americana* Root Stem Powder

*Ekere, Nwachukwu Romanus; Chukwu, Chioma Sarah; Mbaeze, Blessing Chidiebere, and Ihedioha, Janefrances Ngozi.

[a]*Department of Pure and Industrial Chemistry, University of Nigeria Nsukka, Enugu State, Nigeria*

***corresponding author: nwachukwu.ekere@unn.edu.ng**

Abstract

The ability of carbonized and modified avocado (*Persea americana*) root stem powder (C-PA and M-PA) to remediate Cadmium (Cd (II)) and Zinc (Zn (II)) contamination in aqueous solution was studied by varying the carbonization temperature, particle size of the adsorbent, adsorption temperature, pH of the solution, contact time, adsorbent dose and adsorbate concentration. Scanning electron microscopy (SEM), Fourier transform infrared (FTIR) spectroscopy, and X-ray diffraction (XRD) analyses were employed in characterizing both the C-PA and the M-PA. The removal efficiency of up to 86.9 and 90.8 was observed respectively for Cd (II) and Zn (II) at the optimal conditions. Florry-Huggins, Langmuir, Temkin, Dubinin–Radushkevich and Freundlich models were utilized in explaining the equilibrium isotherm of the sorption, and Florry-Huggins best described Zn (R^2 = 0.999) while Cd was best described by Freundlich isotherm (R^2 = 0.997). The kinetics of the sorption process were assessed and pseudo-first order was the best fit in describing Cd (II) uptake (R^2 = 0.965), while Zn (II) was best fitted to the pseudo-second-order kinetics (R^2 = 0.928). The thermodynamic variables revealed an endothermic sorption process for both adsorbates, with a reduction in spontaneity on temperature increase for Zn (II) while the reverse was observed for Cd (II). A single-stage adsorption experiment was performed using the optimal batch adsorption parameters and the result showed an increase in removal efficiency of up to 99.3 and 97.9 for Cd (II) and Zn (II) respectively.

Keywords: Remediation; adsorbent; isotherms; kinetics; thermodynamics

Introduction

When compared to the natural state of the environment before human involvement, pollution is the adverse change that affects a component of the environment due to essential industrial human activity (Al-Taai, 2021). Recently, groundwater quality has been noted to be on a daily decrease due to industrial activities and urbanization. Upon discharge, untreated industrial and domestic wastewater contributes to groundwater pollution (Saha et al., 2017). Wastewater from various industries like metal plating, paper, fertilizer, and pesticides have been observed to contain some amounts of heavy metals (Mansour et al., 2020). Metals like Pb, Cr, Cd, and Zn are persistent contaminants because of their mobility, solubility, and non-biodegradability (Gholami et al., 2020).

Cadmium (Cd) is non-essential, poisonous, and of both human and environmental contamination threat. Cd is naturally present in the environment and emitted from industrial activities (Friberg et al., 2019; Genchi et al., 2020). Cadmium has been classified by both the International Agency for Research on Cancer (IARC) and the United States Environmental Protection Agency (US EPA) as a human carcinogen (Jebril et al., 2022; USEPA, 2023). The major route of Cd exposure is ingestion and inhalation. It is heavily absorbed from contaminated water, food, and air. Cd accumulates in oysters, crabs, kidneys, liver, cocoa beans, mushrooms, and oil seeds (Satarug, 2018). Calcium bio-accumulates and has shown a rather long half-life of about 10-33 years in humans. Prolonged exposure to calcium has been linked to lung and prostate cancer, and renal failure (Idrees et al., 2018).

Zinc (Zn) is the 24th most available element on earth. It is a trace element that is needed by all living things, including plants. Zn is needed for maximum plant growth and development as it is a cofactor of enzymes, a component of proteins, and a component of many enzymes (Broadley et al., 2007). Zn makes up two-thirds of the Earth's surface and this relative abundance makes zinc a persistent environmental pollutant (Sankhla et al.,

2016; Singh Sankhla et al., 2019; Sonone et al., 2021). Although zinc is needed for optimal human body functioning, exposure to high zinc concentrations has been linked to numerous health defects such as hypertension, atrial stroke, genetic mutation, dizziness, headache, and tiredness (Nriagu, 2011; Singh Sankhla et al., 2019).

Groundwater metal contamination is of widespread concern. Recent research has focused on the formulation of cost-effective methods for the cleanup of metallic contaminants in aqueous solutions (Song et al., 2017). Such methods that involve immobilizing contaminants include adsorption, precipitation, and complex formation (Liu et al., 2018). Some agricultural materials have shown good adsorptive capabilities for heavy metals. Plant materials and waste like rice husks, date seeds, sugarcane bagasse, plant root, etc have been applied in the adsorption of heavy metals and other compounds of interest (Francisco et al., 2019; Li et al., 2016; Liu et al., 2018; Mansour et al., 2020; Zulkania et al., 2018).

In this study, Avocado (*Persea americana*) stem bark powder was prepared from the plant material, carbonized, and tested for adsorption capabilities. The impacts of carbonization temperature, particle size, temperature of adsorption, time, pH, adsorbent dose, and adsorbate concentration on the uptake percentage were assessed. The obtained equilibrium data was interpreted using Van't Hoff's thermodynamics model and kinetics and isotherm models. The carbonized *Persea americana* (C-PA) stem bark powder was modified by treatment using ethylenediamine tetraacetic acid (EDTA), and the adsorption was repeated using the observed optimal batch adsorption conditions. The equilibrium concentration was then compared with the ones obtained using the C-PA.

Materials and Methods

Preparation of adsorbent (C-PA)

The *Persea americana* stem bark was collected from a farm in Enugu, Nigeria. It was rigorously washed with double-deionized water and oven-dried at 200 ^{o}C for 1 hr. The dried plant material was allowed to cool, then carbonized in a muffled furnace at varying temperatures of 300, 350, 400, and 450 ^{o}C as described by Ekere et al., (2018). The C-PA was pulverized and sieved into different sizes using 250, 355, and 500 µm mesh sizes.

Modification of the adsorbent

The modification study used the C-PA with the optimal carbonization temperature and particle size. The C-PA was modified following the method reported by Francisco *et al.* (2019). The C-PA (8 g) and EDTA (0.5 g) were mixed in 300 ml of 1 M sodium hydroxide solution at 70 ^{o}C for 3 hrs. The mixture was filtered and air-dried, and the modified adsorbent (M-PA) was utilized for this study.

Preparation of Zn (II) and Cd (II) solutions

The working solutions for the study were prepared from the analytical grade 1000 ppm stock solutions of the respective metals procured from Sigma Aldrich. The various concentrations of Zn (II) and Cd (II) were formulated by serially diluting the stock solution.

Characterization of adsorbent

Infrared spectra analyses of C-PA and M-PA were performed using Buck Scientific M530 FTIR in the 4,000 - 600 cm-1 range. The morphologies of the C-PA and M-PA were observed using Quanta FEG 450 (APOLLO X-EDAX) SEM instrument. The diffraction studies were performed using a Philips m110 XRD instrument.

Batch adsorption studies

Batch-type adsorption studies were performed on the C-PA to determine the particle size, carbonization temperature, adsorption temperature, pH, adsorbate concentration, and adsorbent dose that affords the optimal uptake of the Zn (II) and Cd (II) ions. These parameters have been observed to affect the capacity of the adsorbent to take up metal ions from the solution (Hassan et al., 2020; Jia et al., 2019; Muslim et al., 2022; Suhendrayatna et al., 2019; Xu et al., 2022). The method adopted in a study by Gusain et al., (2021) was employed in carrying out the batch studies.

The impact of particle size was investigated using C-PA particle sizes of 250, 355, and 500 µm. The effect of carbonization temperature to accessed using C-PA carbonized at 300, 350, 400, and 450 ^{o}C. The influence of adsorption temperature was assessed at temperatures of 30, 50, 70, and 90 ^{o}C. The effect of pH was assessed at values of 3, 5, 7, and 9. The impact of the initial Zn (II) and Cd (II) concentrations was assessed at concentrations of 10, 20, 30, 40, and 50 mg/L. The impact of C-PA dose on the uptake of Zn (II) and Cd (II) was assessed at C-PA doses of 0.2, 0.4, 0.6, and 0.8 g.

The solutions were filtered using Whatman (No. 45) filter paper, and the filtrates were analyzed for residual metal ions with a Thermo Scientific iCE 3000 atomic absorption spectrophotometer (AAS). The batch-type investigations were conducted in duplicates and the mean values were recorded.

The levels of Zn (II) and Cd (II) taken up by a unit mass of the adsorbent (q_e) and the percentage of the metals adsorbed were calculated as given below:

$$\%Removal = \frac{(C_i - C_f)}{C_i} \times 100 \quad (1)$$

$$q_e = \frac{(C_i - C_e) \times V}{m} \quad (2)$$

Where C_f *and* Ci are the final and initial concentrations respectively of Zn (II) and Cd (II) solutions (mg/L), C_e is the concentrations in mg/L of Zn (II) and Cd (II) at equilibrium,

q_e is the mass (mg/g) of the respective metals adsorbed on the C-PA, V is the volume (L) of the adsorbate solution, and m is the amount (g) of C-PA.

Adsorption isotherm studies

Florry-Huggins, Langmuir, Temkin, Dubinin–Radushkevich and Freundlich models were adopted in explaining the sorption isotherm. Ragadhita & Nandiyanto (2021) described the isotherm parameters as follows:

Temkin isotherm

This model recognizes the contribution of the heat of adsorption, which diminishes linearly with the adsorbed molecules' layer coverage. The following equation describes the Temkin adsorption isotherm:

$$q_e = \left(\frac{RT}{b_T}\right)(In\ K_t) + \left(\frac{RT}{b_T}\right)\ln C_e \quad (3)$$

Where: K_t = equilibrium constant = maximum binding energy (L mg^{-1}); and T = kelvin temperature, R = gas constant (8.314 $Jmol^{-1}\ K^{-1}$); b_T = heat dependent Temkin constant (J mol^{-1}).

Freundlich isotherm

Freundlich's model is used to show the adsorption intensity of the adsorbate empirically. It is represented linearly with the equation below:

$$logq_e = logK_f + \frac{1}{n}logC_e \quad (4)$$

Where: C_e and q_e = concentration at equilibrium and adsorbed concentration at any given moment respectively (mg L^{-1}), and q_{max} = highest adsorption capacity (mg g^{-1}).

Langmuir isotherm

Langmuir model denotes the peak capacity of adsorption associated with total coverage of the monolayer on the biosorbent outer surface. It is represented linearly as:

$$\frac{C_e}{q_e} = \frac{1}{Q_m K_L} + \frac{C_e}{Q_m} \quad (5)$$

Where C_e and Q_m are the concentration at equilibrium and adsorbed concentration respectively (mg L^{-1}), q_e represents the adsorbed concentration at any given moment and K_L represents the Langmuir constant (L mg^{-1}).

Dubinin-Radushkevich isotherm (D-R)

This model describes the adsorption of molecules onto heterogeneous adsorbent surfaces. The model is represented with a linear equation as follows:

$$In\ q_e = In\ q_m - D\varepsilon^2 \quad (6)$$

Where: q_e = concentration (mg g^{-1}) of adsorbates per adsorbent weight; D = activity coefficient/adsorption energy (mol^{-2} J^{-2}); q_m = adsorption capacity (mg g^{-1}); and ε = adsorbent potential as denoted as:

$$\varepsilon = RTln\left(1 + \frac{1}{C_e}\right) \quad (7)$$

Where: C_e = concentration at equilibrium (mg L^{-1}); T = kelvin temperature; and R = ideal gas constant ($Jmol^{-1}$ K^{-1}). The constants q_m and D were estimated from the intercept and the slope of the graph of $In\ q_e$ and ε^2.

Flory-Huggins model (F-H)

The extent of covering of the surface of the adsorbent by adsorbates is described by the Flory-Huggins' (F-H) isotherm. The linearized Flory-Huggins expression is:

$$\ln\left(\frac{\theta}{C_o}\right) = \ln k_{FH} + n\ ln(1-\theta) \quad (8)$$

$$\theta = 1 - \frac{C_e}{C_o} \quad (9)$$

Where: θ = extent of coverage of the surface, n = amount of adsorbates on sorption sites, and K_{FH} is the F-H equilibrium constant ($Lmol^{-1}$), C_o and C_e = initial and equilibrium adsorbate concentrations respectively.

Adsorption kinetics

The adsorption mechanism and the uptake rate were studied using the intra-particle diffusion model (IPD), pseudo-second-order model (PSO), and pseudo-first-order (PFO) model.

Intra-particle diffusion (IPD)

The IPD model is expressed linearly as shown below:

$$q_t = K_{diff} t^{0.5} + C \quad (10)$$

Where: q_t = adsorbed concentration (mg/g), C = intercept, K_{diff} = IPD factor (mg/g min $^{0.5}$), and t = time (min). From concentration versus time data, q_t is obtained for different agitation times.

Pseudo-second order model (PSO)

The linearized PSO equation is expressed as:

$$1/(q_e - q_t) = 1/q_e + Kt \quad (11)$$

Where: K = PSO constant (g/mg/min), q_e = adsorbed equilibrium concentration (mg/g), t is time (min), and q_t = uptake concentration at time t (mg/g).

Pseudo-first-order (PFO)

The PFO equation is given below:

$$\log(q_e - q_t) = \log q_e - k_1/2.303 \quad (12)$$

Where: k_1 = PFO constant (g/mg/min), t = time (min), qe = adsorbed equilibrium concentration (mg/g), and q_t = uptake concentration at time t (mg/g).

Thermodynamics

This is used to estimate other parameters related to the sorption process like the entropy change (ΔS), Gibb's free energy change (ΔG), and enthalpy change (ΔH). The expressions for these parameters are given below:

$$\Delta G = -RTIn\,K \quad (13)$$

$$K = {}^{q_e}\!/_{C_e} \quad (14)$$

$$\Delta G = \Delta H - T\Delta S \quad (15)$$

Where: T is kelvin temperature, R is gas constant, q_e = adsorbed equilibrium concentration (mg/L), and C_e = concentration at equilibrium (mg/L).

Results and discussions

Characterization of C-PA and M-PA

Different characterization procedures were adopted to assess the adsorption potentials of both C-PA and M-PA. The characterization methods employed are X-ray diffraction (XRD), Scanning electron microscope (SEM), and Fourier Transform Infrared Spectroscopy (FTIR).

FTIR

The constituent functional groups in both C-PA and M-PA were assessed and the resultant spectra were presented in Figure 1. In the spectra of both C-PA and M-PA, the following peaks were observed: peaks corresponding to N-H stretch at 3363 cm^{-1} for C-PA and 3416 – 3313 cm^{-1} for M-PA, indicating the additional amine groups and a successful modification, C-H asymmetric stretch at 2950 cm^{-1} and 2962 cm^{-1} respectively, O-CH_3 stretch at 2836 cm^{-1} and 2767 cm^{-1}, peaks at 2058 cm^{-1} and 2063 cm^{-1} assigned to SCN stretch, C=O stretch of amides between 1616 – 1919 cm^{-1}, C-O stretch at 1182 cm^{-1} and

1106 cm^{-1}, and peaks between 708 – 854 cm^{-1} assigned to COOH stretch. Also observed separately for the adsorbents is a peak at 1302 cm^{-1} which is assigned to CN stretch for C-PA and peaks at 1340 cm^{-1} assigned to P=O stretch and 2597 cm^{-1} assigned to SH stretch for M-PA.

SEM

The morphologies of the carbonized (C-PA) and modified (M-PA) *Persea amercana* (PA) root stem powder were investigated to assess the surface characteristics. The C-PA in Figure 1a was observed to be of smooth surface with pockets for the potential intake of metal ions. On modification, shiny spots were observed on M-PA alongside a rougher surface as can be seen in Figure 1b, which indicates successful adherence of the additional components (likely the amine groups from the EDTA) onto the PA. These additional groups could potentially increase the attraction of the adsorbate ions for the adsorbent surface.

XRD

The diffraction pattern of both the C-PA and M-PA were studied and presented in Figure 2. The XRD data for C-PA showed that a predominantly amorphous form of carbon is present in C-PA with a bit wide peaks at an angle of 2θ: 22^o – 32^o. A similar peak was also observed in M-PA at an angle of about 2θ: 27^o, accompanied by a sharp peak at 2θ: 49.52^o indicating the introduction of crystallinity into the PA adsorbent on modification with EDTA.

Batch adsorption studies

Particle size

The impact of particle size of the C-PA on the percentage uptake of the adsorbate ions was assessed and illustrated in Figure 4a. The percentage uptake of the adsorbates was

noted to decrease with an increase in the particle size. An optimal percentage uptake was observed at 250 µm particle size for Zn (II) and Cd (II). This trend is confirmed by the works of Ekere et al. (2016) who reported that it could be linked to increased surface area. Comparatively, a higher percentage uptake was observed for Cd (61.7) than for Zn (55.9) at the optimal particle size.

Carbonization temperature

The impact of the carbonization temperature on the uptake of Zn (II) and Cd (II) into C-PA was assessed and the result is illustrated in Figure 4b. The percentage uptake was linear until an optimal value was attained at a temperature of 450 ^{O}C. This suggests that the PA requires a high temperature of up to 450 ^{O}C for activation. This temperature dependence was uniform for the sorption of Cd (II) and Zn (II), and this observation could be ascribed to the accessibility of more internal pores of the PA bio-sorbent for adsorption (Ekere et al., 2018). Cd (II) showed a higher percentage uptake of 59.9 at the optimal temperature than Zn (47.7).

Initial concentration of Zn (II) and Cd (II)

The impact of the initial concentration of Zn (II) and Cd (II) on the percentage uptake of the metal ions was assessed and the result is illustrated in Figure 4c. The percentage uptake was observed to rise linearly with increasing Zn (II) and Cd (II) concentrations until equilibrium was attained at 40 ppm Zn (II) and Cd (II) levels. Monier et al. (2010) made a similar observation and suggested that this may be the result of accelerated collision between the adsorbate ions and the adsorbent on increasing metal ion concentration, which subsequently results in increased adsorbate uptake. Cd (II) showed a higher percentage uptake of 77.2 at the optimal concentration compared to Zn (69.9).

Effect of pH

The impact of pH on the uptake of Zn (II) and Cd (II) by the C-PA was assessed and the result is illustrated in Figure 4d. It was noted that the range of pH between 5>pH<5 was unfavorable for the uptake of Zn (II) and Cd (II) onto C-PA. Optimal uptake of Zn (II) and Cd (II) was observed at pH 5. The percentage uptake of Zn (II) and Cd (II) increased with an increase in pH until an optimum was observed at a pH of 5. This may be due to the electrostatic interactions between the C-PA surface and the metal ion solution as well as the higher amount of H_3O^+ competing with the metal ions at lower pH. The percentage uptake reduced above pH 5 due to the precipitation of Zn (II) and Cd (II) ions at rising pH values (Mansour et al., 2020; Pranata Putra et al., 2014).

Effect of Dose

The impact of C-PA dosage on the percentage uptake of Zn (II) and Cd (II) was assessed and the result is depicted in Figure 4e. The percentage uptake was observed to increase linearly with increased C-PA dose until an optimum was attained at an adsorbent dose of 0.6 g. This trend could be linked to a rise in the number of vacant positions for sorption with an increasing amount of C-PA (Ameh et al., 2023; Ekere et al., 2018). C-PA was better in the removal of Cd (II) at the optimal dose than for Zn (II) as evidenced by the observed percentage uptakes of 54.5 and 37.2 for both adsorbates respectively.

Effect of Time

The influence of equilibration time on the percentage uptake of Zn (II) and Cd (II) by the C-PA was assessed and the result displayed in Figure 4f revealed that maximum percentage uptake of the adsorbates onto the C-PA was achieved at an equilibration time of 50 and 30 minutes for Zn and Cd respectively. The decrease in the percentage uptake of the adsorbates after optimal time could be as a result of saturation of the available

positions on the C-PA. Similar variations with time have also been reported for heavy metals in prior studies (Muslim et al., 2022; Nursiah et al., 2023; Suhendrayatna et al., 2019). Equilibrium percentage uptake of 68.2 and 86.4 was observed for Zn (II) and Cd (II) respectively.

Effect of Temperature

The impact of temperature on percentage uptake of Zn (II) and Cd (II) by the C-PA was assessed and the result presented in Figure 4g showed linear adsorption until an optimal temperature of 50 ^{o}C and 70 ^{o}C for Zn (II) and Cd (II) respectively. This trend could be attributed to the temperature requirement for the activation of the C-PA and is in agreement with the reports of Onwordi et al. (2019) and Rout et al. (2009). The percentage uptake at the optimal equilibration temperature for Cd (II) and Zn (II) was observed to be 86.9 and 90.8 respectively.

Isotherm studies

Five isotherm models were used to interpret the behavior of the Cd (II) and Zn (II), and the suitability of each model was assessed by comparing the regression (R^2) values. The models employed are the Florry-Huggins, Temkin, Freundlich, Dubinin–Radushkevich, and Langmuir models. The parameters and the plots are displayed in Table 1 and Figure 5. The data presented revealed that Freundlich model best described the uptake of Cd (II) unto the C-PA as evidenced by the R^2 value of 0.997 indicating a heterogeneous surface adsorption. The adsorption intensity constant (n) which indicates the favorability of the sorption process was calculated as 0.979 for Cd (II), indicating a favorable adsorption. This is supported by the work of Jimoh et al. (2015). On the other hand, the Florry-Huggins model with an R^2 value of 0.999 was the best fit to explain the uptake of Zn (II), and the positive Gibb's free energy (ΔG) estimated from the equilibrium constant (K_{F-H})

showed that the process was but unspontaneous and endothermic. This observation also agrees with the reports of Chaba & Nomngongo (2019).

Kinetic studies

Three kinetic models were employed to assess the speed of the equilibration between Cd (II) and Zn (II). The models are intraparticle diffusion (IPD), pseudo-second-order (PSO), and pseudo-first-order (PFO) models. The model parameters are presented in Table 2. The suitability of each model in describing the rate of equilibration was assessed based on the regression (R^2) values. The sorption of Cd (II) was found to be best fitted to PFO, followed by IPD as is evidenced by the respective R^2 values of 0.965 and 0.954 showing that the rate of the sorption process is dependent on both the particle size of the C-PA and the interaction between Cd (II) and the adsorbent surface (Manjuladevi et al., 2018). Zn (II) on the other hand was found to be best described by PSO. This was similarly observed by Manal et al., (2017).

Thermodynamics studies

To further understand the impact of temperature in the sorption of Cd (II) and Zn (II), thermodynamic variables of the process such as enthalpy change (ΔH), entropy change (ΔS), and Gibb's free energy change (ΔG) were determined and shown in Table 3. The results showed that a positive entropy value was observed for Cd (II) indicating some degree of disorderliness at the surface of adsorbate and adsorbent, and some level of attraction for C-PA (Jimoh et al., 2015). Zn (II) on the other hand showed a negative entropy value, indicating less disorderliness and a lesser level of attraction for C-PA.

A positive value for enthalpy (ΔH) points to an endothermic sorption process while a negative value shows an exothermic process. Likewise, a positive value below 84 KJ/mol suggests the possibility of physical adsorption while values above suggest chemical adsorption (Iftekhar et al., 2017). The positive enthalpy (ΔH) values observed for Zn (II)

and Cd (II) indicate endothermic sorption for both adsorbates with Cd (II) exhibiting chemisorption and Zn (II) physisorption.

Overall, the values of Gibb's free energy (ΔG), which is a measure of the spontaneity of the sorption process, were observed to become more positive for Zn (II) on the increase in temperature indicating a less spontaneous sorption process on increase in temperature (Din et al., 2014). Cd (II) on the other hand showed increasingly negative ΔG values on an increase in temperature, supporting the higher temperature dependency observed in the batch studies. Bazrafshan et al., (2015) also noted a similar observation in their study on bio-sorption of cadmium.

Modification studies

The *Persea americana* bio-sorbent was modified using the disodium salt of Ethylenediamine tetraacetic acid (EDTA) to improve the adsorptive properties and adsorption studies were repeated on the adsorbates of interest using the optimal parameters observed in the initial studies (pH = 6, Time = 30 mins, Initial Concentration = 40 ppm, Adsorbent dose = 0.6 g, Temperature = 50 and 70 ^{o}C). The percentage uptake of the adsorbates is presented in Table 4.

The modification of the C-PA with EDTA greatly increased the uptake of Zn (II) and Cd (II) as the percentage uptake superseded the levels observed in the batch adsorption studies. This observed improvement in the percentage after modification with EDTA is also supported by similar studies conducted by Ezzeddine et al., (2023) and Francisco et al., (2019). It is also noteworthy that the modification also resulted in improved temperature efficiency for Cd (II) as a higher percentage uptake was noted at a lower temperature of 50 ^{o}C

Conclusion

This study assessed the capacity of a cheap and environmentally friendly agricultural material C-PA, for the effective remediation of Zn (II) and Cd (II) from aqueous solutions. The batch experiment showed that C-PA could serve as an efficient bio-sorbent for the remediation of Cd (II) and Zn (II). The experimental data was fitted to various isotherm models and the interaction of Cd (II) with C-PA was best fitted to Freundlich isotherm, while the interaction with Zn (II) was best described by the Florry-Huggins isotherm. The adsorption kinetics for the uptake of Cd (II) was best described by PFO while that of Zn (II) was best described by PSO. The observed ΔH values indicate an endothermic sorption process for both Cd (II) and Zn (II). Modification of C-PA with EDTA was effected and the adsorption studies were repeated at the optimal batch conditions. The result showed an enhanced percentage uptake of 97.9 and 99.3 for Zn and Cd respectively. Overall, this study revealed that both C-PA and M-PA are excellent bio-sorbents for the immobilization and subsequent remediation of Zn (II) and Cd (II) from aqueous solution.

Funding: The authors did not use external funding for this work

Conflict of interest: No conflict of interest was observed by the authors

Ethical approval: Not applicable

Data availability: All data related to this research are included in this manuscript

References

Al-Taai, S. (2021). ph. *IOP Conference Series: Earth and Environmental Science*, *790*, 12026. https://doi.org/10.1088/1755-1315/790/1/012026

Ameh, O. M., Chahul, H. F., & Ike, D. C. (2023). *Evaluation of the Adsorption and Corrosion Inhibition Effects of Piliostigma thonningii Extract on Mild Steel in 1 . 0 M Hydrochloric Acid*. *14*(1), 97–112.

Bazrafshan, E., Zarei, amin allah, & Mostafapour, F. (2015). Biosorption of cadmium from aqueous solutions by Trichoderma fungus: kinetic, thermodynamic, and equilibrium study. *Desalination and Water Treatment*, *57*, 1–11. https://doi.org/10.1080/19443994.2015.1065764

Broadley, M. R., White, P. J., Hammond, J. P., Zelko, I., & Lux, A. (2007). Zinc in plants. *New Phytologist*, *173*(4), 677–702. https://doi.org/10.1111/j.1469-8137.2007.01996.x

Chaba, J. M., & Nomngongo, P. N. (2019). Effective adsorptive removal of amoxicillin from aqueous solutions and wastewater samples using zinc oxide coated carbon nanofiber composite. *Emerging Contaminants*, *5*, 143–149. https://doi.org/10.1016/j.emcon.2019.04.001

Din, M. I., Hussain, Z., Mirza, M. L., Shah, A. T., & Athar, M. M. (2014). Adsorption optimization of lead (II) using Saccharum bengalense as a non-conventional low cost biosorbent: isotherm and thermodynamics modeling. *International Journal of Phytoremediation*, *16*(7–12), 889–908. https://doi.org/10.1080/15226514.2013.803025

Ekere, N. R., Agwogie, A. B., & Ihedioha, J. N. (2016). Studies of biosorption of Pb2+, Cd2+ and Cu2+ from aqueous solutions using Adansonia digitata root powders. *International Journal of Phytoremediation*, *18*(2), 116–125. https://doi.org/10.1080/15226514.2015.1058329

Ekere, N. R., Agwogie, A. B., & Ihedioha, J. N. (2018). Removal of of pb(II), cd(II), cu(II) and ni(II) ions from aqueous solution using pentaclethra macrophylla stem activated carbon. *Pakistan Journal of Analytical and Environmental Chemistry*, *19*(2), 195–204. https://doi.org/10.21743/pjaec/2018.12.21

Ezzeddine, Z., Abdallah, L., & Hamad, H. (2023). Heavy Metals Adsorption on Cyanex-272 Modified Activated Carbon: Efficacy and Selectivity. *Universal Journal of Carbon Research*, *1*(1), 22–37. https://doi.org/10.37256/ujcr.1120231937

Francisco, N., Hugo, B., & San Jose, J. (2019). The Potential of EDTA – Modified Rice Husk Ash as Solid Phase Extraction Resin in Seawater. *Global Scientific Journal*, *7*(1), 187 – 199. https://www.globalscientificjournal.com/researchpaper/The_Potential_of_EDTA_Modified_Rice_Husk_Ash_as_Solid_Phase_Extraction_Resin_in_Seawater.pdf

Friberg, L., Kjellström, T., Elinder, C.-G., & Nordberg, G. F. (2019). *Cadmium and health: a toxicological and epidemiological appraisal* (L. Friberg, T. Kjellström, C.-G. Elinder, & G. F. Nordberg (eds.); 1st Editio). CRC Press. https://doi.org/10.1201/9780429260599

Genchi, G., Sinicropi, M., Lauria, G., Carocci, A., & Catalano, A. (2020). The Effects of Cadmium Toxicity. *International Journal of Environmental Research and Public Health*, *17*, 3782. https://doi.org/10.3390/ijerph17113782

Gholami, L., Rahimi, G., & Khademi Jolgeh Nezhad, A. (2020). Effect of thiourea-modified biochar on adsorption and fractionation of cadmium and lead in contaminated acidic soil. *International Journal of Phytoremediation*, *22*(5), 468–481. https://doi.org/10.1080/15226514.2019.1678108

Gusain, D., Bux, F., Dubey, S., & Sharma, Y. C. (2021). Batch Adsorption Process of

Metals and Anions for Remediation of Contaminated Water. In *Batch Adsorption Process of Metals and Anions for Remediation of Contaminated Water* (Issue March). https://doi.org/10.1201/9781003006367

Hassan, M., Liu, Y., Naidu, R., Parikh, S. J., Du, J., Qi, F., & Willett, I. R. (2020). Influences of feedstock sources and pyrolysis temperature on the properties of biochar and functionality as adsorbents: A meta-analysis. *The Science of the Total Environment*, *744*, 140714. https://doi.org/10.1016/j.scitotenv.2020.140714

Idrees, N., Tabassum, B., Abd Allah, E. F., Hashem, A., Sarah, R., & Hashim, M. (2018). Groundwater contamination with cadmium concentrations in some West U.P. Regions, India. *Saudi Journal of Biological Sciences*, *25*(7), 1365–1368. https://doi.org/10.1016/j.sjbs.2018.07.005

Iftekhar, S., Srivastava, V., & Sillanpää, M. (2017). Enrichment of lanthanides in aqueous system by cellulose based silica nanocomposite. *Chemical Engineering Journal*, *320*, 151–159. https://doi.org/https://doi.org/10.1016/j.cej.2017.03.051

Jebril, N. M., Boden, R., & Braungardt, C. (2022). THE GROUNDWATER CONTAMINATED WITH CADMIUM: A SYSTEMATIC REVIEW. *ANBAR JOURNAL OF AGRICULTURAL SCIENCES*, *20*(2), 483–494. https://doi.org/10.32649/ajas.2022.176912

Jia, L., Fan, B. G., Li, B., Yao, Y. X., Huo, R. P., Zhao, R., Qiao, X. L., & Jin, Y. (2019). Effects of pyrolysis mode and particle size on the microscopic characteristics and mercury adsorption characteristics of Biomass Char. *BioResources*, *13*(3), 5450–5471. https://doi.org/10.15376/biores.13.3.5450-5471

Jimoh, A. ., Adebayo, G. B., Otun, K. O., Ajiboye, A. T., Bale, A. T., Jamiu, W., & Alao, F. O. (2015). *Bior emediation & Biodegradation Sorption Study of Cd (II) from Aqueous Solution Using Activated Carbon Prepared from Vitellaria*

paradoxa Shell. *6*(3). https://doi.org/10.4172/2155-6199.1000288

Li, Q., Chen, B., Lin, P., Zhou, J., Zhan, J., Shen, Q., & Pan, X. (2016). Adsorption of heavy metal from aqueous solution by dehydrated root powder of long-root Eichhornia crassipes. *International Journal of Phytoremediation*, *18*(2), 103–109. https://doi.org/10.1080/15226514.2014.898017

Liu, H., Xu, F., Xie, Y., Wang, C., Zhang, A., Li, L., & Xu, H. (2018). Effect of modified coconut shell biochar on availability of heavy metals and biochemical characteristics of soil in multiple heavy metals contaminated soil. *The Science of the Total Environment*, *645*, 702–709. https://doi.org/10.1016/j.scitotenv.2018.07.115

Manal, L., Leila, Y., & Achour, S. (2017). Removal of Zinc from Water by Adsorpion on Bentonite and Kaolin. *ATHENS JOURNAL OF SCIENCES*, *4*, 47–58. https://doi.org/10.30958/ajs.4-1-4

Manjuladevi, M., Anitha, R., & Manonmani, S. (2018). Kinetic study on adsorption of Cr(VI), Ni(II), Cd(II) and Pb(II) ions from aqueous solutions using activated carbon prepared from Cucumis melo peel. *Applied Water Science*, *8*(1), 36. https://doi.org/10.1007/s13201-018-0674-1

Mansour, R. A., Atef, R., Elazaby, R. R., & Zaatout, A. A. (2020). Experimental study on the adsorption of Cr+6 and Ni+2 from aqueous solution using low-cost natural material. *International Journal of Phytoremediation*, *22*(5), 508–517. https://doi.org/10.1080/15226514.2019.1683716

Monier, M., Ayad, D. M., & Sarhan, A. A. (2010). Adsorption of Cu(II), Hg(II), and Ni(II) ions by modified natural wool chelating fibers. *Journal of Hazardous Materials*, *176*(1), 348–355. https://doi.org/https://doi.org/10.1016/j.jhazmat.2009.11.034

Muslim, A., Purnawan, E., Nasrullah, Meilina, H., Azwar, M. Y., Deri, N. O., & Kadri, A. (2022). Adsorption of Copper Ions Onto Rice Husk Activated Carbon Prepared Using Ultrasound Assistance: Optimization Based on Step-By-Step Single Variable Knockout Technique. *Journal of Engineering Science and Technology*, *17*(4), 2496–2511.

Nriagu, J. (2011). Zinc Toxicity in Humans. In *Encyclopedia of Environmental Health* (pp. 801–807). https://doi.org/10.1016/B978-0-444-52272-6.00675-9

Nursiah, C., Desvita, H., Elviani, E., Farida, N., Muslim, A., Rosnelly, C. M., Mariana, M., & Suhendrayatna, S. (2023). Adsorbent Characterization from Cocoa Shell Pyrolysis (Theobroma cacao L) and its Application in Mercury Ion Reduction. *Journal of Ecological Engineering*, *24*(6), 366–375. https://doi.org/10.12911/22998993/163167

Onwordi, C., Uche, C., Emmanuel, A., & Petrik, L. (2019). Comparative study of the adsorption capacity of lead (II) ions onto bean husk and fish scale from aqueous solution. *Journal of Water Reuse and Desalination*, *9*. https://doi.org/10.2166/wrd.2019.061

Pranata Putra, W., Kamari, A., Najiah Mohd Yusoff, S., Fauziah Ishak, C., Mohamed, A., Hashim, N., & Md Isa, I. (2014). Biosorption of Cu(II), Pb(II) and Zn(II) Ions from Aqueous Solutions Using Selected Waste Materials: Adsorption and Characterisation Studies. *Journal of Encapsulation and Adsorption Sciences*, *04*(01), 25–35. https://doi.org/10.4236/jeas.2014.41004

Ragadhita, R., & Nandiyanto, A. B. D. (2021). How to calculate adsorption isotherms of particles using two-parameter monolayer adsorption models and equations. *Indonesian Journal of Science and Technology*, *6*(1), 205–234. https://doi.org/10.17509/ijost.v6i1.32354

Rout, K., Mohapatra, M., Mohapatra, B. K., & Anand, S. (2009). *Pb (II), Cd (II) and Zn (II) adsorption on low grade manganese ore*. *1*(1), 106–122.

Saha, P., Shinde, O., & Sarkar, S. (2017). Phytoremediation of industrial mines wastewater using water hyacinth. *International Journal of Phytoremediation*, *19*(1), 87–96. https://doi.org/10.1080/15226514.2016.1216078

Sankhla, M. S., Kumari, M., Nandan, M., Kumar, R., & Agrawal, P. (2016). Heavy Metals Contamination in Water and their Hazardous Effect on Human Health-A Review. *International Journal of Current Microbiology and Applied Sciences*, *5*(10), 759–766. https://doi.org/10.20546/ijcmas.2016.510.082

Satarug, S. (2018). Dietary Cadmium Intake and Its Effects on Kidneys. *Toxics*, *6*(1). https://doi.org/10.3390/toxics6010015

Singh Sankhla, M., Kumar, R., & Prasad, L. (2019). *Zinc Impurity in Drinking Water and Its Toxic Effect on Human Health*. *17*, 84. https://doi.org/10.5958/0974-4487.2019.00015.4

Song, B., Zeng, G., Gong, J., Liang, J., Xu, P., Liu, Z., Zhang, Y., Zhang, C., Cheng, M., Liu, Y., Ye, S., Yi, H., & Ren, X. (2017). Evaluation methods for assessing effectiveness of in situ remediation of soil and sediment contaminated with organic pollutants and heavy metals. *Environment International*, *105*, 43–55. https://doi.org/10.1016/j.envint.2017.05.001

Sonone, S. S., Jadhav, S., Sankhla, M. S., & Kumar, R. (2021). Water Contamination by Heavy Metals and their Toxic Effect on Aquaculture and Human Health through Food Chain. In *Letters in Applied NanoBioScience* (Vol. 10, Issue 2, pp. 2148–2166). AMG Transcend Association. https://doi.org/10.33263/LIANBS102.21482166

Suhendrayatna, S., Abdurrahman, A., & Elvitriana, E. (2019). Study on the optimization

of mercury ion (II) adsorption with activated carbon from a biomass combination of palm bunches and rice husk. *Aceh International Journal of Science and Technology*, *8*, 161–168. https://doi.org/10.13170/aijst.8.3.15160

USEPA. (2023). *What are the trends in waste and their effects on human health and the environment?* EPA's Report on the Environment (ROE). https://www.epa.gov/report-environment

Xu, W., Liu, C., Zhu, J. M., Bu, H., Tong, H., Chen, M., Tan, D., Gao, T., & Liu, Y. (2022). Adsorption of cadmium on clay-organic associations in different pH solutions: The effect of amphoteric organic matter. *Ecotoxicology and Environmental Safety*, *236*(April), 113509. https://doi.org/10.1016/j.ecoenv.2022.113509

Zulkania, Ariany, Hanum, Ghina F., & Sri Rezki, Amelia. (2018). The potential of activated carbon derived from bio-char waste of bio-oil pyrolysis as adsorbent. *MATEC Web Conf.*, *154*, 1029. https://doi.org/10.1051/matecconf/201815401029

Table 1: Regression data and isotherm constants for adsorption of Zn (II) and Cd (II) onto C-PA

Figures

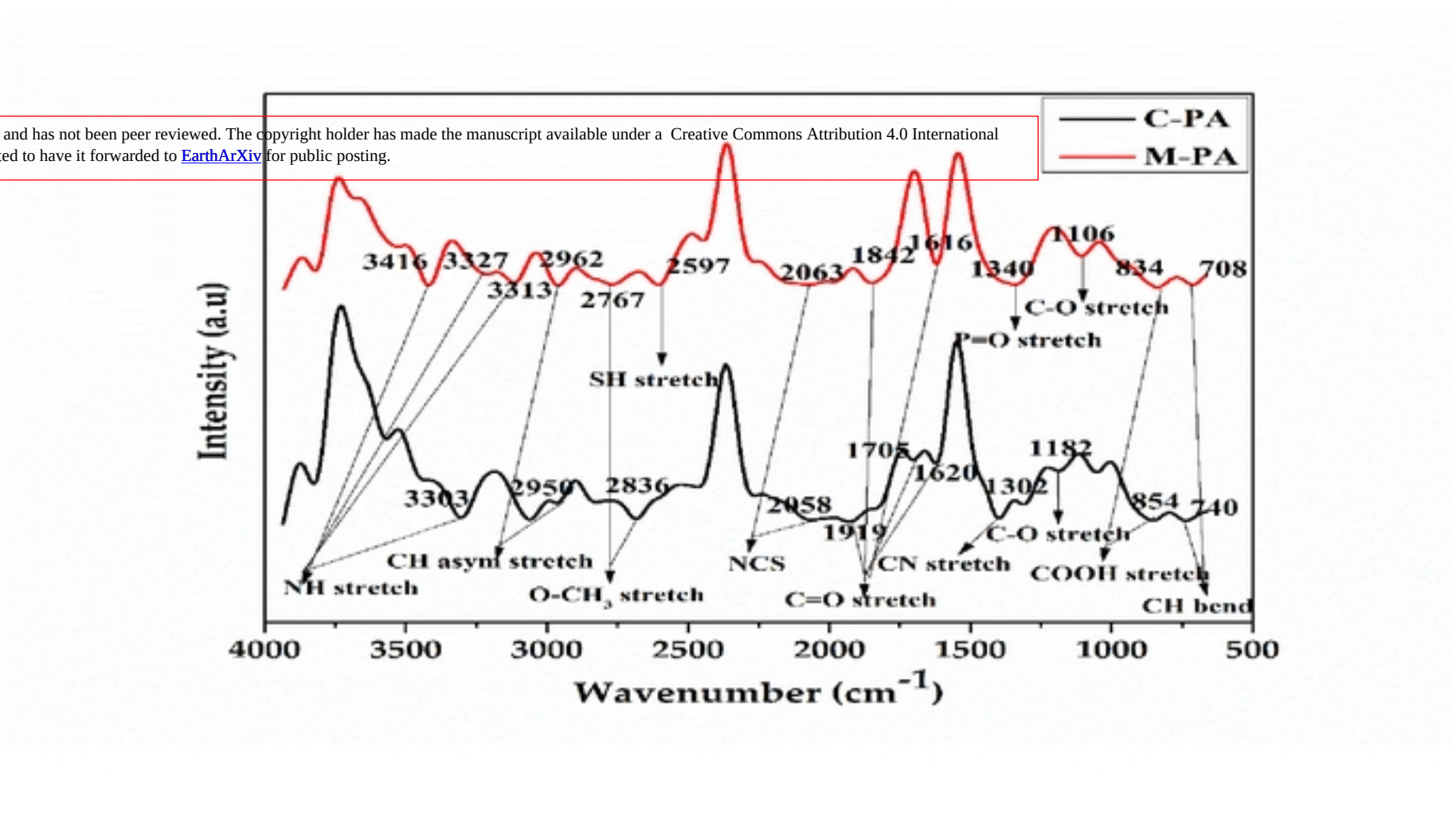

Figure 1: FTIR spectra of C-PA and M-PA

(a) C-PA

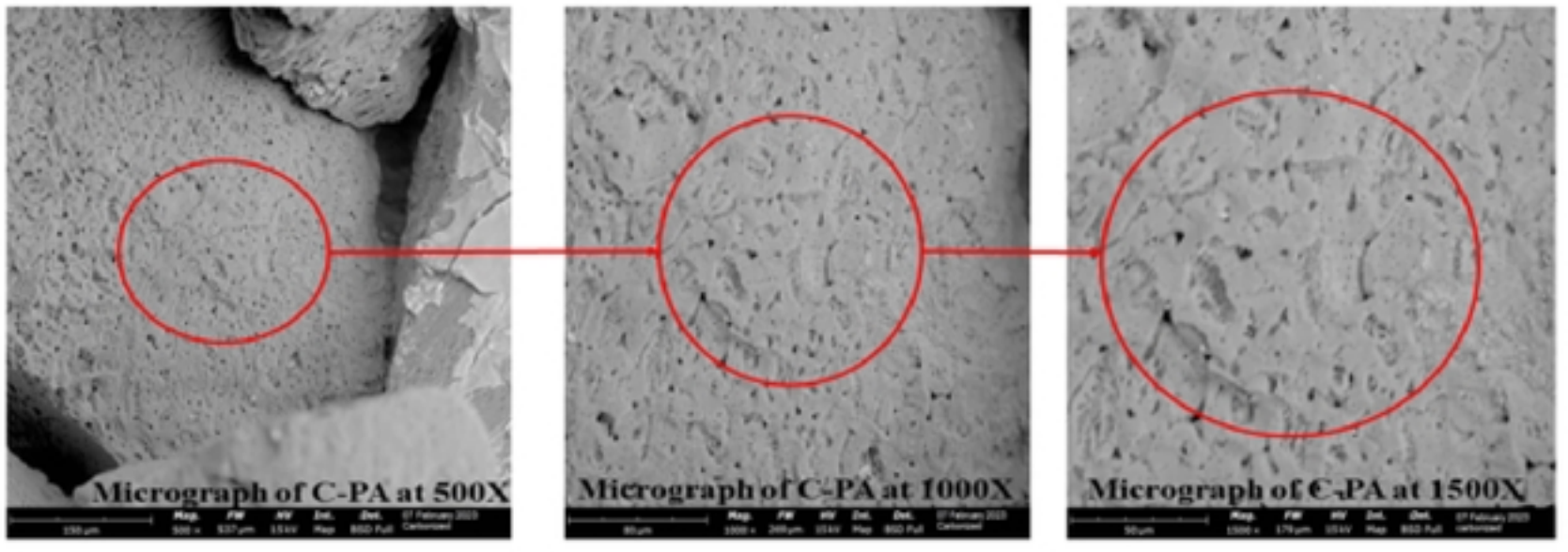

(b) M-PA

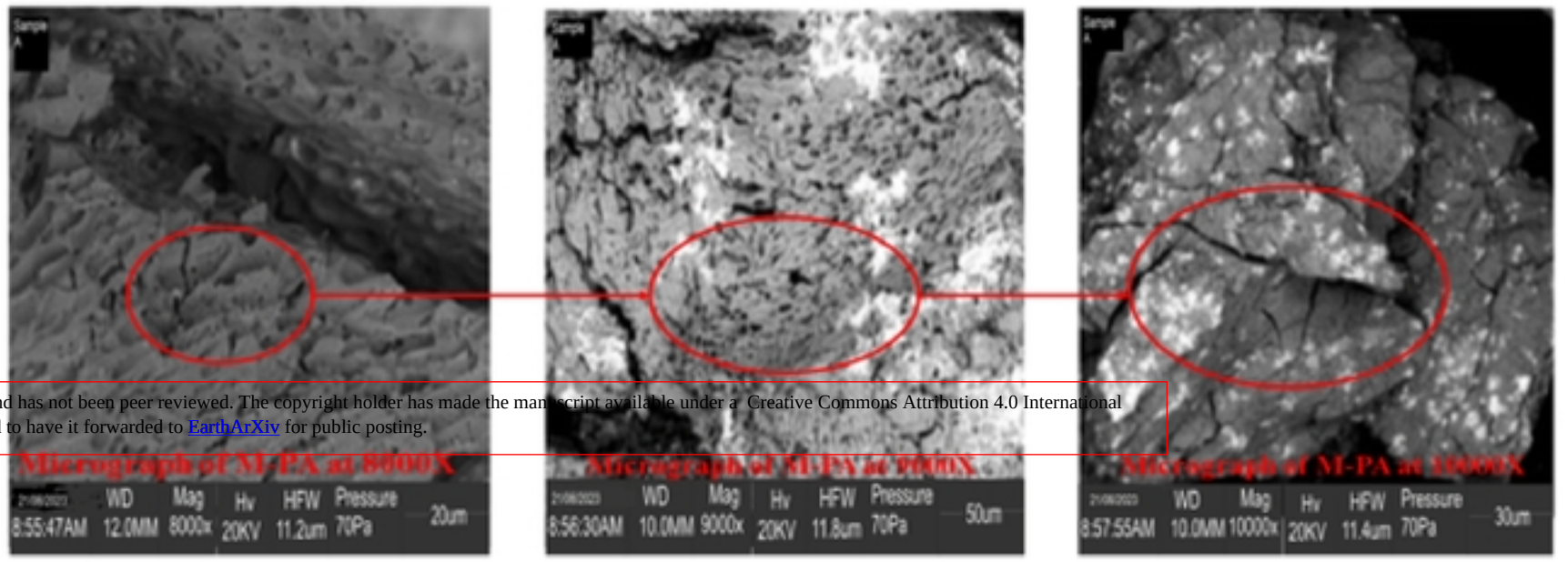

Figure 2: Micrographs of the PA adsorbent on carbonization (a), and on modification (b)

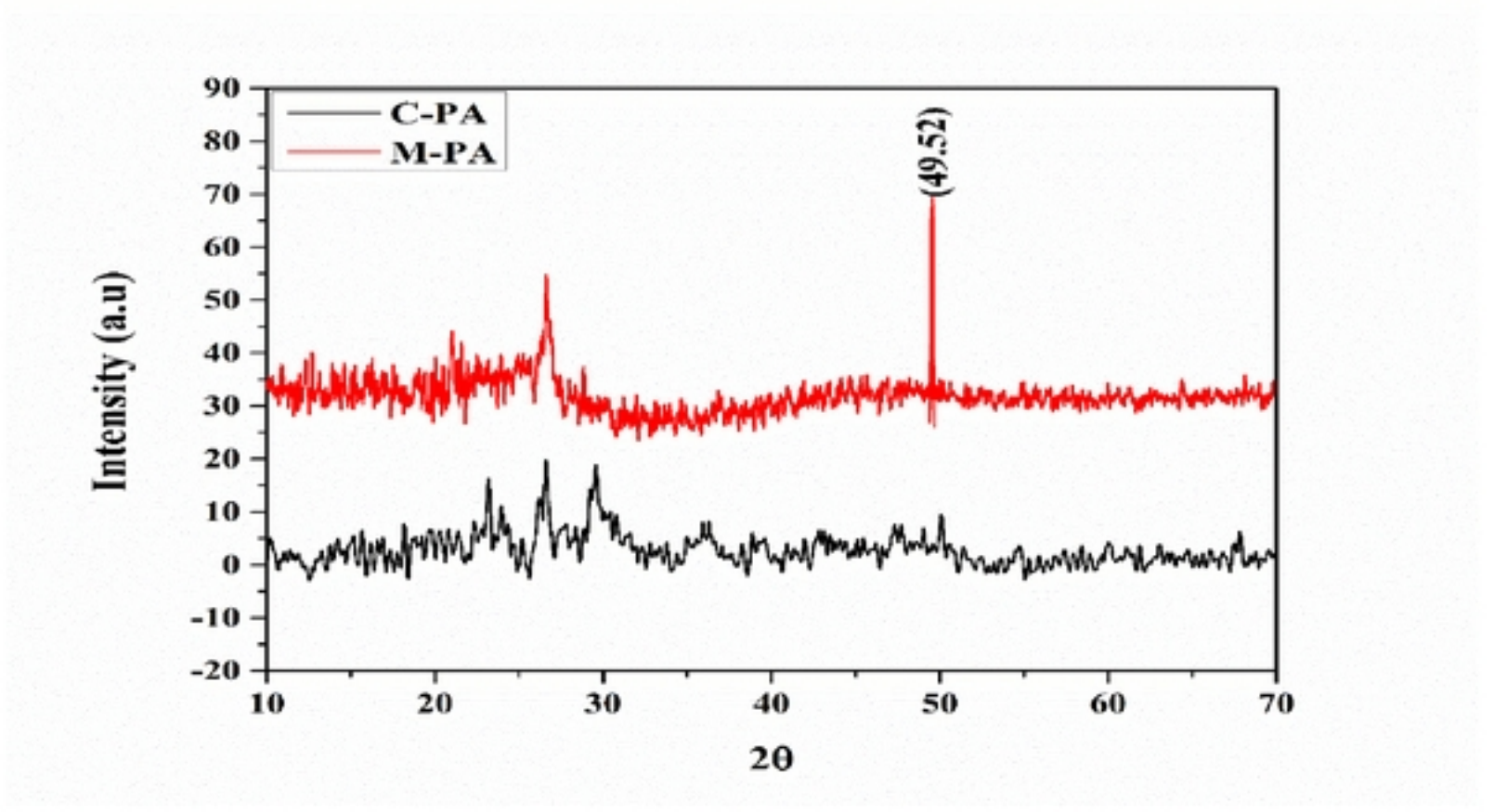

Figure 3: XRD graph of C-PA and M-PA

(a)

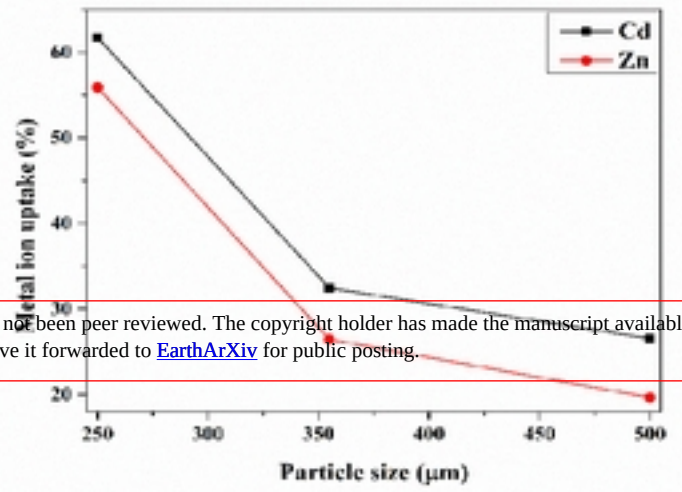

(b)

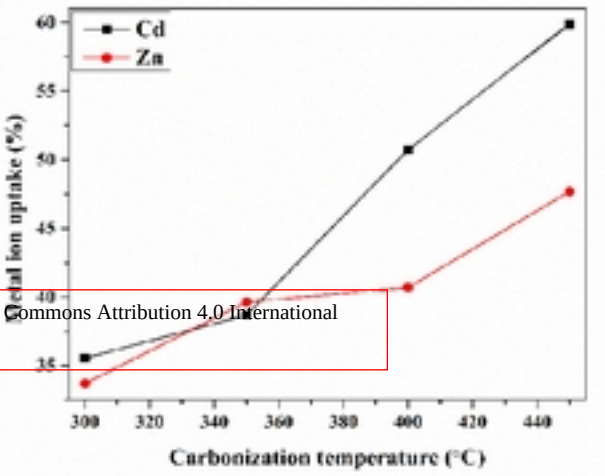

c)

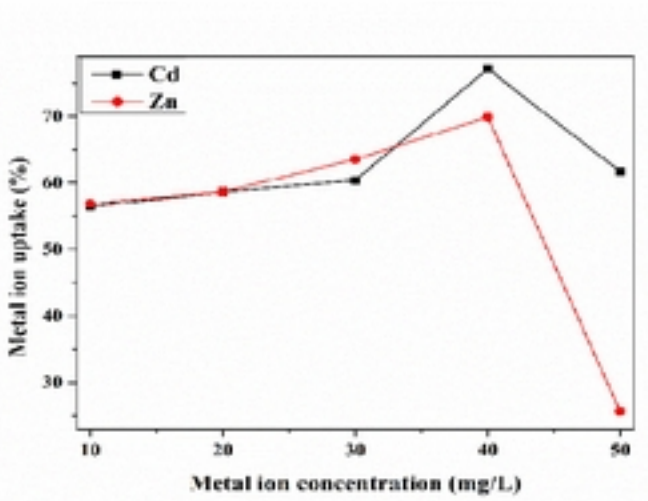

d)

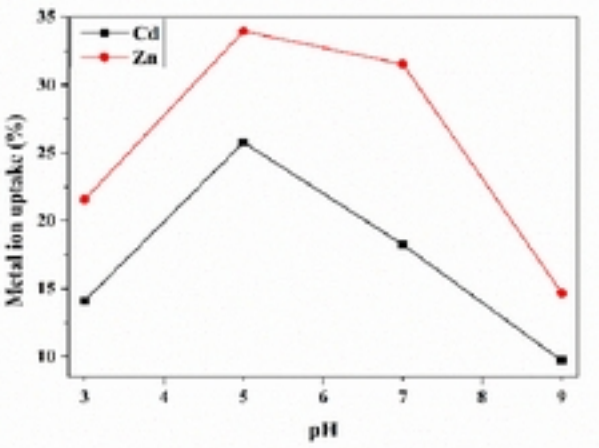

e)

f)

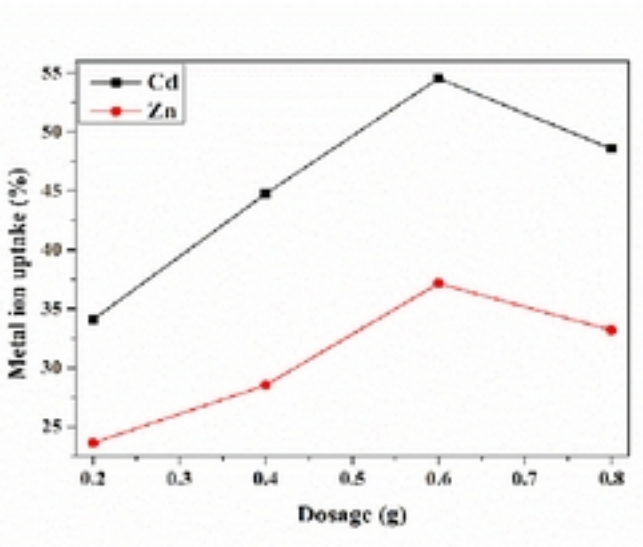

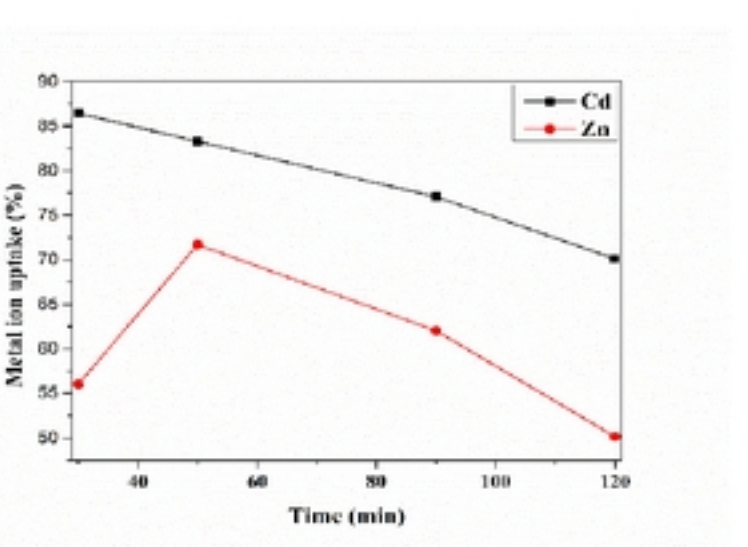

g)

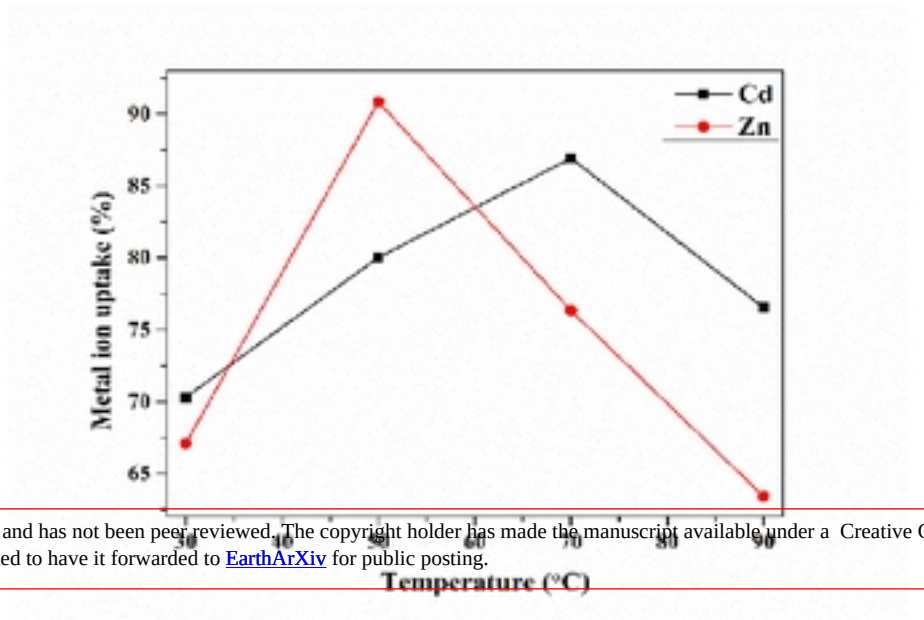

Figure 4: Effect of batch adsorption parameters on the percentage uptake of Cd (II) and Zn (II). (a) particle size, (b) carbonization temperature, (c) adsorbate concentration, (d) pH, (e) dose, (f) time, and (g) temperature

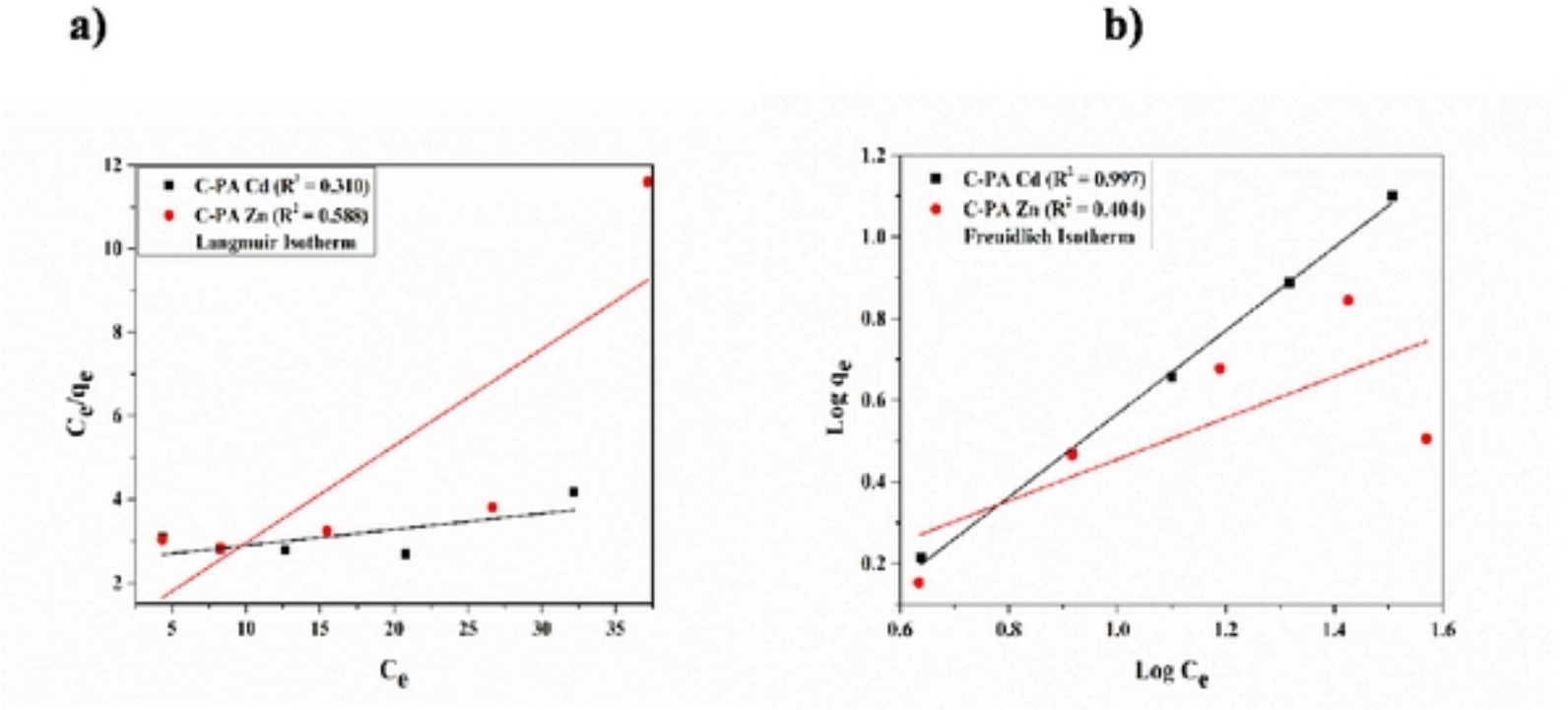

c)

d)

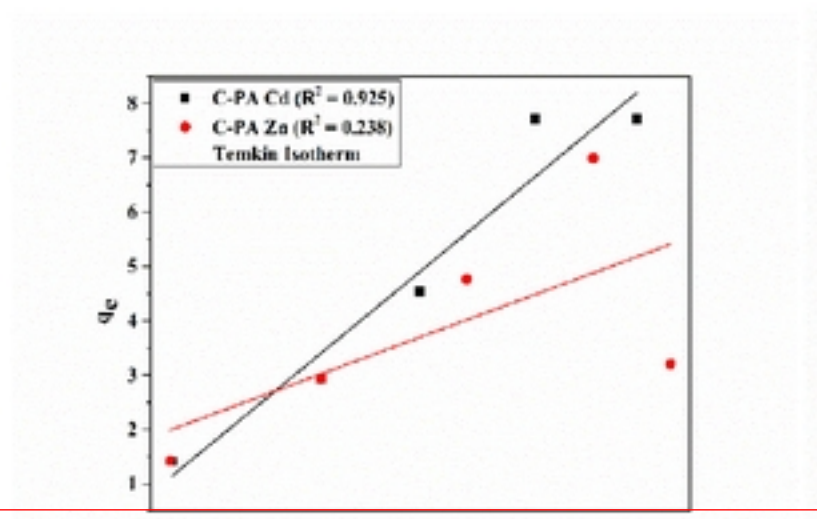

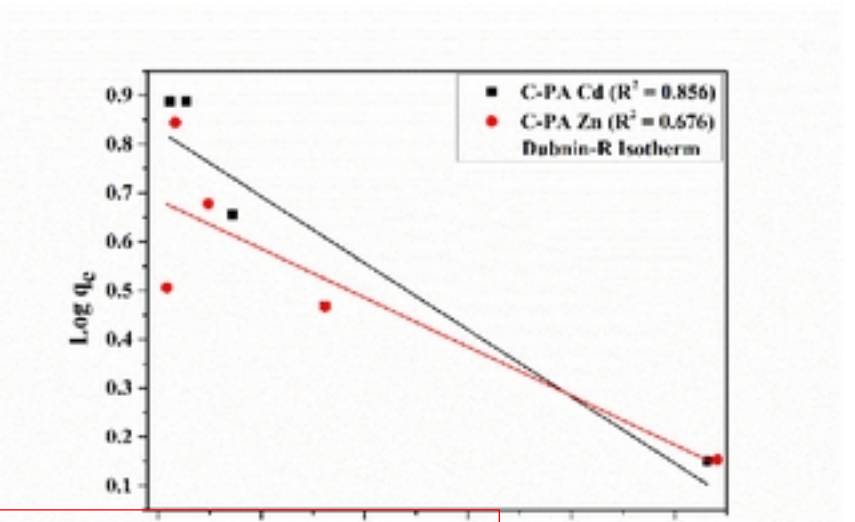

e)

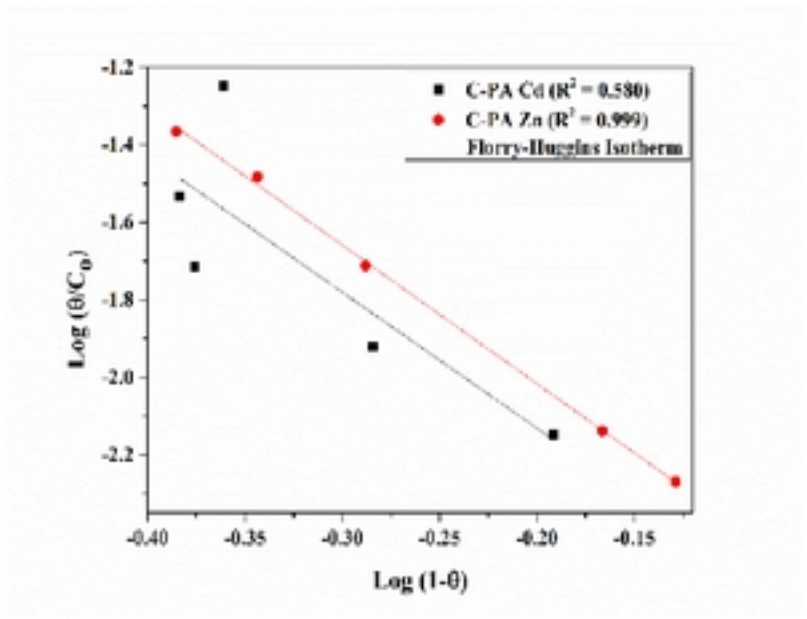

Figure 5: Plots of isotherm models for the uptake of Zn (II) and Cd (II) onto the C-PA. (a) Langmuir (b) Freundlich (c) Temkin (d) Dubinin–Radushkevich (e) Florry-Huggins

(a) (b)

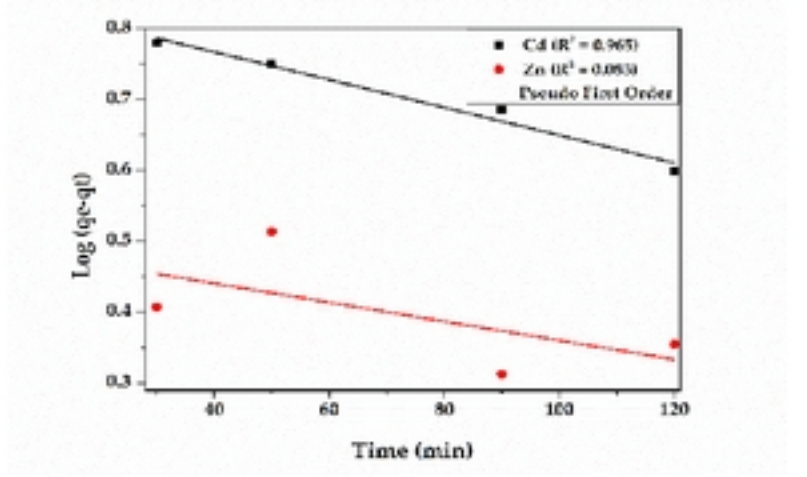

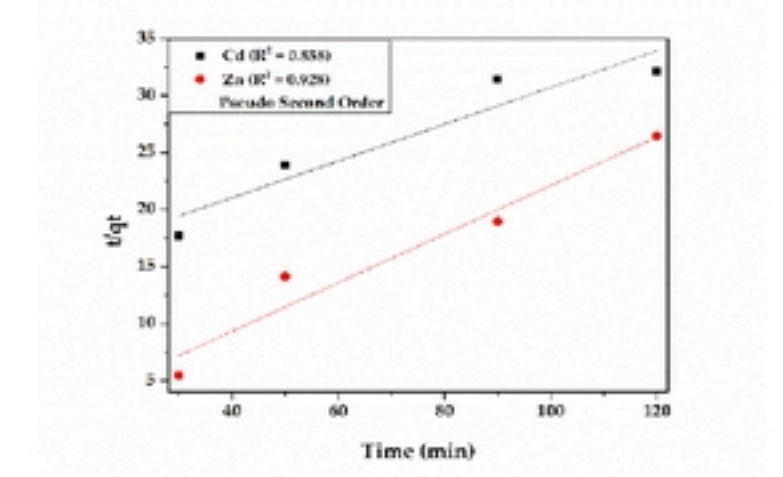

(c)

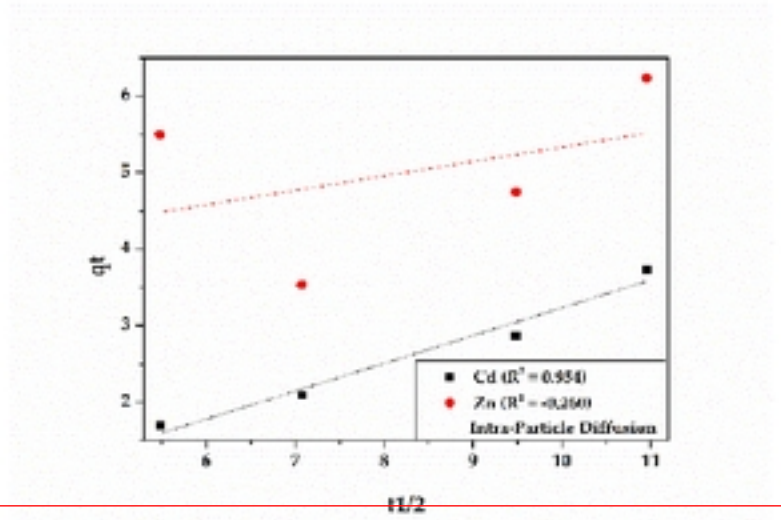

Figure 6. Plots of Kinetic Models for the sorption. (a) PFO; (b) PSO; (c) IPD